JOURNAL OF GUIDANCE, CONTROL, AND DYNAMICS
Vol. 17, No. 4, July–August 1994

Zero-Gyro Safemode Controller for the Hubble Space Telescope

F. Landis Markley*
NASA Goddard Space Flight Center, Greenbelt, Maryland 20771
and
John D. Nelson†
Lockheed Missiles and Space Company, Inc., Sunnyvale, California 94088

A safehold mode has been implemented for Hubble Space Telescope that ensures a power-positive and thermally safe state without the use of rate gyros. This paper presents an overview of this Zero-Gyro Sunpoint safemode, followed by details of the algorithm, the control system design, and results of simulations and of an on-orbit test of the algorithm.

Introduction

ZERO-GYRO Sunpoint (ZGSP) is a safemode that permits the Hubble Space Telescope (HST) to function without gyros. HST was launched with six primary high-accuracy single-degree-of-freedom gyros for redundancy. The science pointing mode of HST normally uses four gyros to provide gyro fault detection and improved smoothing of gyro noise, but good pointing performance (with reduced fault detection capability) is possible with three gyros.[1-4] However, some type of contingency mode is required in case four of the six primary gyros are incapacitated, because the body rate perpendicular to the input axes of the remaining two gyros is unobservable.

If four of the six primary gyros are lost, vehicle health and safety can still be maintained with the hardware sunpoint capability using the Pointing and Safemode Electronics Assembly along with the Retrieval Mode Gyro Assembly, a set of backup lower-accuracy gyros designed to allow sunpoint until the primary gyros can be brought on line (after replacement if necessary). The retrieval mode gyros have a limited operational life, however, so it is undesirable to rely on these gyros for long-term control. Although there is no reason to doubt good hardware sunpoint performance, it was felt that an additional gyroless safemode resident in the HST flight computer was a reasonable precaution. The gyroless safemode concept was conceived after gyro 6 and then gyro 4 failed during the 1st year of HST operation. The ZGSP design was based on the normal software sunpoint (SWSP) safemode,[4,5] because of the critical margins on flight computer memory and throughput, as well as the rapid development schedule. Development of this safemode algorithm went from concept to flight code in 3 months, with uplink to HST on January 20, 1992. When uplinked, ZGSP was intentionally disabled by removing all paths to it in the software.

Gyro 1 ceased producing rate data on November 18, 1992, reducing the gyro error detection capability, as mentioned above. Thus, the system momentum test,[6] which was developed in conjunction with ZGSP, was activated on November 20. A decision was also made to enable the ZGSP safemode, but only after performing an on-orbit test of this mode. The test was performed on January 26–27, 1993, and the ZGSP safemode was enabled on January 30, 1993, following a full evaluation of the test results.

The following sections contain an overview of the ZGSP algorithm; and then, after a brief discussion of the HST coarse Sun sensors, a detailed discussion of the algorithm. Presentations of a linear stability analysis of the algorithm and of its simulated performance follow, and the paper concludes with a detailed discussion of the planning and results of the on-orbit test of the safemode.

Zero-Gyro Sunpoint Algorithm Overview

ZGSP pointing control uses coarse Sun sensors (CSS) and the magnetic sensing system (MSS) as attitude sensors. The ZGSP algorithm uses much of the existing SWSP processing. Requirements for ZGSP are the same as SWSP safemode and can be simply stated as the ability to perform Sun capture and maintain sunpointing indefinitely without ground commanding. The reaction wheel assembly is used for primary attitude control in both modes, and magnetic torquers are used for momentum management.

While HST is in sunlight, ZGSP uses CSS data for position and rate information about axes perpendicular to the Sun line and the magnetic field vector for rate damping about the Sun line. The magnetometer-derived rates are inaccurate because Earth's magnetic field is not inertially fixed, but they are useful in keeping the rates around the Sun line at an acceptably low level. When in shadow, all three axes drift, but the drift away from the Sun line is limited by a momentum bias in the direction of the sunpointing axis. The momentum bias is built up in the reaction wheels using the magnetic torquers during sunlit portions of the orbit after the Sun has been seen once inside a database-specified CSS deadband.

The ZGSP mode is a robust, long-term safemode. No ephemeris information is required. Maneuvers during initial capture are performed by open-loop acceleration commands. The aperture door is always closed at ZGSP entry to preclude the possibility of Sun down the boresight during the initial capture. Attitude knowledge is lost because of rotation around the Sun line; therefore, the high-gain antennas are not used in ZGSP.

Figure 1 shows the definition of HST vehicle axes. The precise definition of the axes is in relation to the fine guidance sensors, but they can be approximately thought of as $V1$ along

This contains material from two different presented papers: Paper 92-4613 at the AIAA Guidance, Navigation, and Control Conference, Hilton Head, SC, Aug. 10–12, 1992; and Paper 93-3831 at the AIAA Guidance, Navigation, and Control Conference, Monterey, CA, Aug. 9–11, 1993; received July 31, 1992; revision received Oct. 1, 1993; accepted for publication Oct. 15, 1993.

* Assistant Head, Guidance and Control Branch, Code 712. Associate Fellow AIAA.
†Group Engineer. Member AIAA.

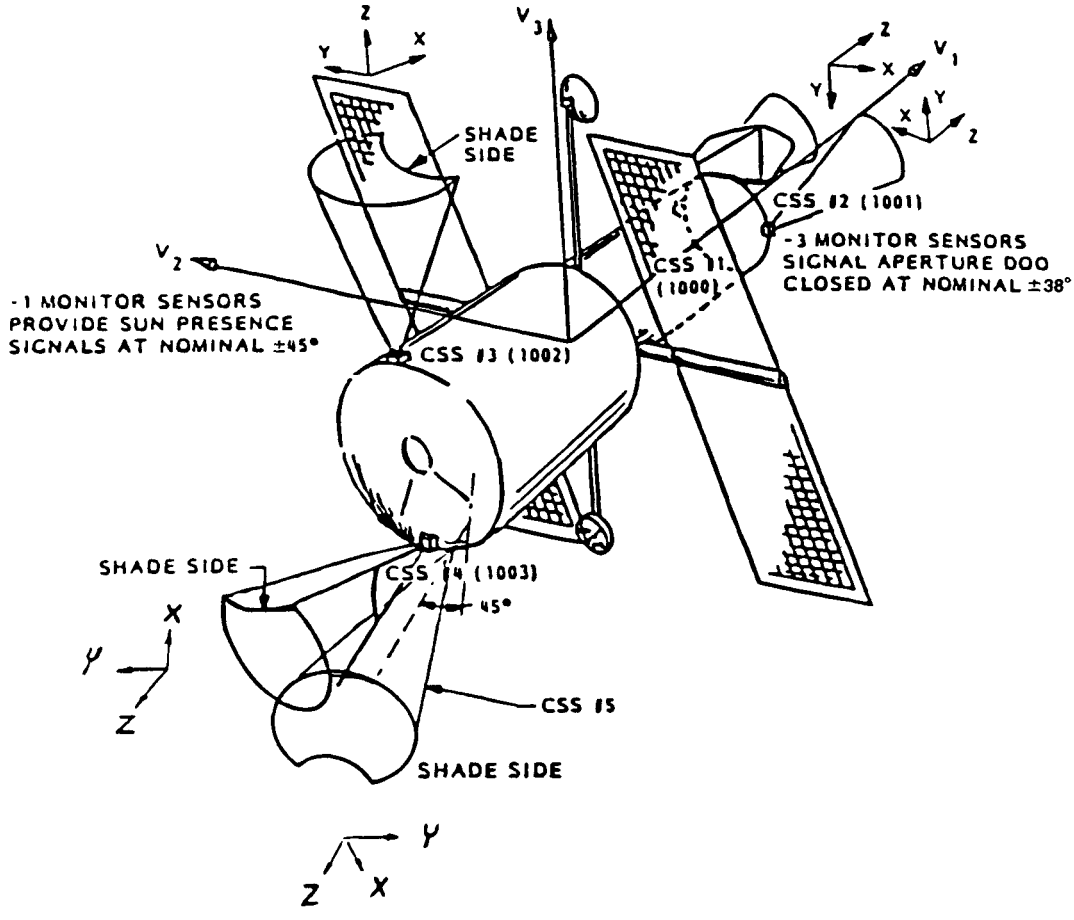

Fig. 1 HST coordinate frame and CSS fields of view.

the telescope boresight, $V2$ along the solar array rotation axis, and $V3$ to complete the orthogonal triad.

The ZGSP algorithm supports either $V3$ or $-V1$ sunpoint in the same manner as the SWSP mode. Because ZGSP and SWSP use the same software flags and code for this computation, the selection of sunpoint axis is automatically the same for both safemodes. This precludes any possibility of a large capture should a transition from SWSP to ZGSP be necessary. The sunpoint axis can be selected autonomously onboard or can be selected by the Space Telescope Operations Control Center (STOCC). If autonomous selection is used, the vehicle is maneuvered to establish either $V3$ or $-V1$ sunpointing depending upon which axis is closer to the Sun line. This ensures that the smallest possible maneuver is performed. If STOCC selection is enabled, the vehicle is maneuvered so that the STOCC-selected axis is driven to the Sun line. In either case, the solar arrays are rotated to the appropriate position orthogonal to the Sun, and the sunpointing axis is never changed autonomously after it has been selected. Thermal considerations make it undesirable to maintain HST at a $-V1$ sunpointing attitude for extended periods of time. Thus, the $V3$ axis is currently STOCC-selected, and the on-orbit tests were performed for this selection only.

Activation and operation of ZGSP are divided into several phases, including the following: 1) initial Sun check; 2) $V2$ maneuver, if required; 3) control of axes perpendicular to Sun line for Sun inside final CSS field of view; 4) control of axis along Sun line for Sun inside final CSS field of view; 5) momentum bias control; and 6) eclipse control. Steps 1 and 2 are needed only during the initial sunpoint capture. More detail on each step follows.

Coarse Sun Sensor Description

An understanding of the CSS system is necessary in order to understand the ZGSP safemode. Each of the five CSSs on HST includes three identical monitor sensors and two control sensors. Vehicle coordinate axes and orientations of the CSSs are shown in Fig. 1. Note that CSS 1 and 2 have the same field of view for redundancy along the telescope boresight. Reference 7 provides more detail.

ZGSP uses Sun/no-Sun outputs from the monitor sensors in logic branching and limiter selection. The monitor sensors have a field of view with half-cone angle of ±45 deg on CSSs 3, 4, and 5 and ±38 deg on CSSs 1 and 2. The monitor sensors detect whether or not the Sun is in the field of view and indicate either "Sun present" or "Sun not present." Redundant signals are compared and voted in the software to reduce the possibility of erroneous output.

Each control sensor incorporates a pyramid-shaped detector and produces an x and a y position error. The output characteristic for one axis is shown in Fig. 2. The response curve has a peak at around 45 deg off the sensed axis. This is important for ZGSP because it means that back-differenced control sensor output (i.e., derived rate) will have the correct sign only when the Sun is within 45 deg of that axis. It also means that unusual conditions can result when the Sun is more than 45 deg from one axis (incorrect sign) but less than 45 deg from the other (correct sign). Averaging of the control sensor outputs is performed to smooth the signal. In normal software sunpoint, the output signal is limited to 14 deg in the CSS processing, well inside the linear region. The limit has been raised to 38 deg for ZGSP, so the back-differenced rates have meaningful values over a larger range, and captures occur faster. The back-differenced rates are noisy because of the 0.35-deg bit size of the CSS signal sent to the flight computer, but filtering produces a usable rate measurement.

Zero-Gyro Sunpoint Algorithm Details

This section presents the sequence of steps to capture and maintain sunpointing during ZGSP operations, as discussed in

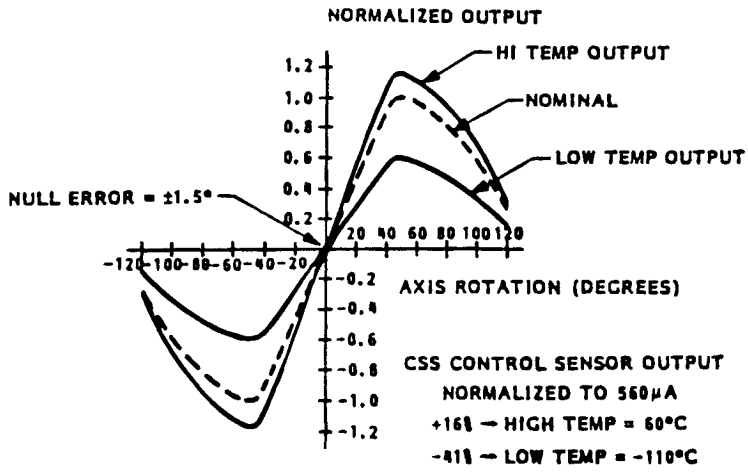

Fig. 2 CSS control sensor characteristic.

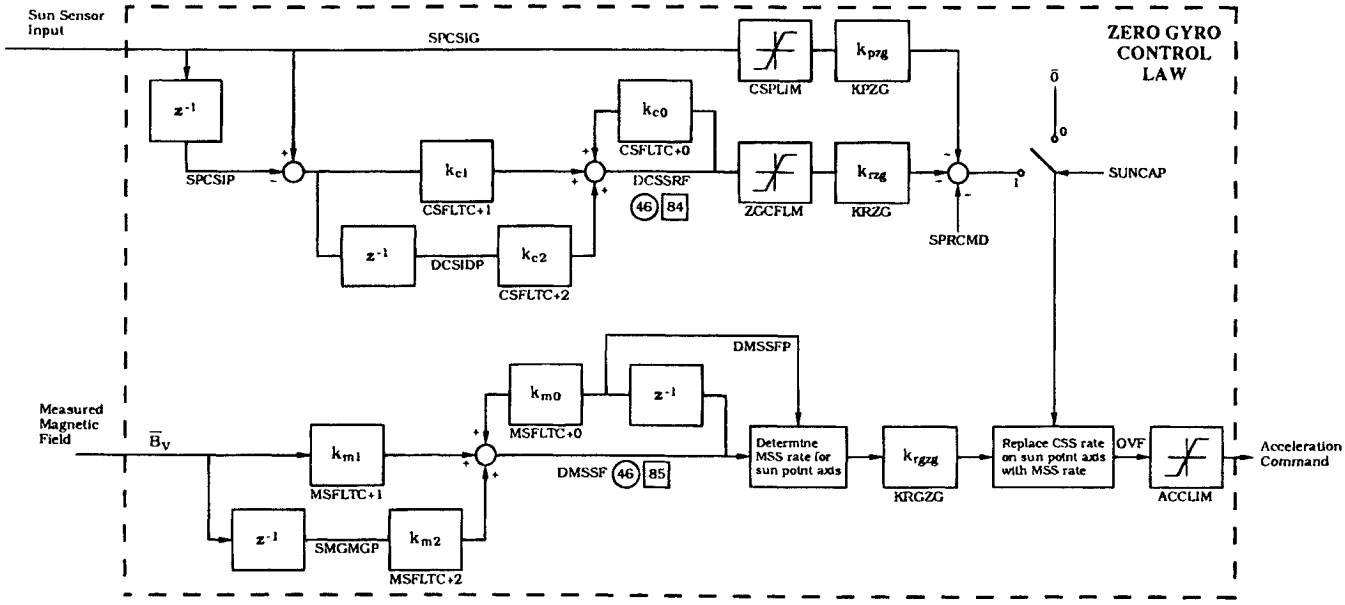

Fig. 3 Zero-Gyro Sunpoint block diagram.

Ref. 8. The details are presented for the $V3$ sunpoint case only. The $-V1$ case is entirely analogous, although CSS 4 (directed along $-V1$) is used as the target CSS instead of CSS 3, and the momentum bias level differs. In most cases, indexing is used in the flight software to avoid duplication of code. Figure 3 shows a block diagram of the ZGSP system. Details of the code and database appear in the Flight Software design specifications.[4,5]

Initial Sun Check

When the sunpoint law is first enabled, an initial Sun check identical to the SWSP Sun check is performed.[4] Coarse Sun sensors 3, 4, 1, 2, and 5 are checked (in that order) for Sun presence. If the Sun is seen by CSS 3, execution of the control algorithms for Sun inside the final CSS field of view is begun immediately. If the Sun is seen by some CSSs but not by CSS 3, a $V2$ maneuver is performed, as described below. If the Sun is not seen by any CSS, the eclipse control described below is executed. If, because of multiple CSS failures, the Sun does not appear in any CSS field of view after a database-specified time interval greater than the longest expected eclipse, a sky sweep maneuver is executed.

V2 Maneuver

The CSS 3 boresight is along the $+V3$ axis. Thus, simultaneously forcing the Sun to the $V1$-$V3$ plane and maneuvering around $V2$ guarantee that the Sun will eventually enter the CSS 3 field of view. The $V2$ maneuver, if required, is performed by applying a constant acceleration bias of the appropriate sign to the $V2$ command. This bias is applied until either the Sun is seen by CSS 3 or a database time limit is reached. Acceleration commands are converted to body torque commands and then to reaction wheel torque commands farther downstream in the 1 Hz processing. The equivalent $V2$ torque magnitude is 0.3 N-m, and the maximum time of torque application is 1,800 s. No other control is applied to the $V2$ axis.

During a $V2$ maneuver, CSS data is processed to produce position and derived rate feedback for the $V1$ and $V3$ axes in order to maneuver the HST to put the Sun in the $V1$-$V3$ plane. Acceleration limits in this step are 0.0000044 rad/s^2 about $V1$ and $V3$, equating to roughly 0.15 and 0.3 N-m respectively. This step is similar to the $V2$ maneuver used in SWSP, but a timed acceleration instead of a rate command is used to slew the spacecraft.

Control of Axes Perpendicular to Sun Line for Sun Inside Final CSS Field of View

CSS 3 measures rotations around $V1$ and $V2$ once the Sun is inside its field of view, so control is switched to produce $V1$ and $V2$ acceleration commands using CSS 3 outputs. Control inside the CSS 3 field of view is divided into two regimes for $V1$ and $V2$: Sun inside and Sun outside the database-sized

deadband, set at 3 deg. When the Sun is within 3 deg of the $V3$ axis, the $V1$ and $V2$ torques are zeroed to reduce control law noise and reaction wheel duty cycle. Outside the deadband, $V1$ and $V2$ are controlled using position and derived rate feedback, as in the $V2$ maneuver. The measured Sun vector is back-differenced and then smoothed with a 0.1-Hz first-order filter to provide rate feedback. Position and acceleration limiters are used to control capture rates and maximum commanded accelerations on $V1$ and $V2$.

A position limiter is used to provide a crude rate-limited capture. The position limit is set at 10 deg prior to the time the Sun is seen inside the deadband. When combined with the position and rate gains, the position limiter gives a capture rate of approximately 0.1 deg. Once the Sun is seen inside the deadband, it is assumed that no more large captures will be needed, because the momentum bias will keep drift during eclipse small. The position limit is then lowered to 2.5 deg, giving a capture rate limit of 0.025 deg/s. Smoothing performed on the CSS-derived rates reduces the magnitude of the computed rate signal, so the actual vehicle rates can be larger.

Although the same control gains are applied whenever the Sun is inside the CSS 3 field of view but outside the deadband, the nonlinear nature of the CSS output signal described above forces use of two acceleration limiters. One limiter is used if the Sun is inside the final monitor field of view (i.e., within 45 deg of the CSS 3 boresight for $V3$ ZGSP) and the other is used outside the final monitor field of view. Because of the incorrect slope of the rate feedback outside the monitor field of view, the rate term is essentially positive feedback. Allowed accelerations are larger inside the final monitor field of view because the back-differenced rate has the correct sign; values are set to the equivalent of 0.56 and 1.1 N-m around the $V1$ and $V2$ axes, respectively. Outside the monitor field of view, the equivalent torques are 0.15 and 0.3 N-m, the same as during the $V2$ maneuver.

Control of Axis along Sun Line for Sun Inside Final CSS Field of View

$V3$ control with the Sun in the CSS 3 field of view is done with rate feedback only using the measured magnetic field to provide a rate estimate. The control is low gain rate damping with a limited torque of 0.3 N-m. The rate about $V3$ is computed from the measured magnetic field, using the simplifying assumption that the Earth's magnetic field and the $V3$ axis are inertially fixed, by

$$\omega_z = (b_y \mathrm{d}b_x/\mathrm{d}t - b_x \mathrm{d}b_y/\mathrm{d}t)/(b_x^2 + b_y^2)$$

where ω_z is the estimated $V3$ rate and b_x and b_y are the $V1$ and $V2$ components of the measured magnetic field. A first-order filter with a break frequency at 0.005 Hz is incorporated to filter the magnetometer outputs prior to use in the above equation.

The resulting derived rates are inaccurate because Earth's magnetic field describes a roughly conical motion at an average rotation rate of two revolutions per orbit caused by spacecraft orbital motion. The 5787-s HST orbit period gives an orbit rate of 1.086×10^{-3} rad/s. Because $V3$ rate damping control tries to keep the projection of the magnetic field in the $V1$-$V2$ plane as stationary as possible, the spacecraft $V3$ rate will exhibit oscillations about zero rate or ± 2 rev/orbit, depending on the orientation of the Sun line with respect to the orbit plane. The rotational motion around $V3$ does not have any effect on Sun pointing; but can affect drift during eclipse, because the net momentum bias can be reduced by the body rates, lowering the stiffening effect of the bias.

Momentum Bias Control

After the Sun has been seen once inside the final CSS deadband, commands to the magnetic torquers are changed to build up a momentum bias in the reaction wheels in order to limit body drift away from the Sun line during the eclipse period of each orbit. This is accomplished by adding a bias to the computation of the total system momentum, causing the magnetic torquers to attempt to drive the computed total momentum back toward zero. The external torque around $V3$ applied by the magnetic torquers is fed forward to the control law, and any residual motion is sensed and controlled. Thus, the added momentum is loaded onto the reaction wheels and does not result in an increase of the spacecraft body rates. The wheel bias approaches the commanded level within a period of about two orbits.

The momentum bias levels were selected as a compromise between reasonable wheel speeds and drift during eclipse. The bias level is 250 N-m-s on $V3$ in $V3$ ZGSP and 200 N-m-s on $V1$ in $-V1$ ZGSP, because the reaction wheel configuration would require higher speeds for a $-V1$ bias of the same magnitude as the $V3$ momentum bias.

The onboard calculation of the system momentum differs from SWSP in that only reaction wheel momentum is included, because the zero-gyro onboard estimate of the spacecraft angular velocity is not accurate enough to be included in the computation. It is assumed that body rates are small once Sun capture is achieved and maintained.

Eclipse Control

The spacecraft is allowed to drift during the eclipse phase, because an inertial reference is not available. No reaction wheel commands are sent, so the internal wheel speed loops maintain each wheel at the speed it had at the time that HST entered eclipse (called Enter Orbit Night). Momentum bias keeps drift away from the Sun line relatively small, but larger than the errors in the inertial hold on gyros used in the SWSP safemode. Another change from SWSP is that ZGSP turns off momentum management during eclipse; no magnetic torquer commands are sent, because no good inertial reference is available.

Zero-Gyro Sunpoint Stability Analysis

The ZGSP system is linear when the Sun is inside the monitor cone of the final CSS. A linear stability analysis shows that the system is extremely stable with a gain margin of 37 dB and a phase margin of 59 deg. Reference 8 contains Bode and Nichols plots for this case. The bandwidth is approximately 0.0029 Hz. Because of the low bandwidth, bending mode effects are negligible.

Simulated Zero-Gyro Sunpoint Performance

A set of 50 simulation cases was run with both $V3$ and $-V1$ ZGSP to check out the final algorithm and database. These cases had a wide variety of initial body rates, wheel speeds, and attitudes. Initial rates as large as 0.2 deg/s on one axis or 0.3 deg/s in a direction making equal angles to the three coordinate axes were simulated. These rates are conservative; they are higher than rates resulting from a gyro failure during a slew. The simulation cases were also rerun with different terminator timing to see whether large rates at Enter Orbit Night could cause a ZGSP failure. Most runs covered 20,000 s (about three orbits). They were examined to verify acceptable capture performance and drift during eclipse.

Performance of $V3$ ZGSP was acceptable in all cases. The longest capture time was 8000 s, although that particular case had nearly captured at Enter Orbit Night after 4000 s. The second longest capture time was 2700 s, and typical capture time was around 1500 s, even with large initial rates. Worst case drift during eclipse was largest during the first eclipse period, because reaction wheel momentum bias was not completely built up. Worst case drifts for the first, second, and third eclipses were 100, 51, and 42 deg, respectively. The largest wheel speed was 3400 rpm, with steady-state speeds around 2000 rpm.

Figures 4–6 show the results of the V3 ZGSP simulation run with a 2700 s capture time and a drift during the first eclipse of 100 deg. The initial body rates were −0.02, 0.06, and −0.08 deg/s along the *V*1, *V*2, and *V*3 axes, respectively. The starting Sun line was 160 deg away from the *V*3 axis. The initial reaction wheel speeds were −500, −243, 171, and 328 rpm.

Figure 4 shows the control flag that indicates the various stages of the control law; the flag is 2 during a *V*2 maneuver, 5 during sunpoint, and 0 when in eclipse. Figure 5 shows the angle between the *V*3 axis and the Sun vector. The capture time in this case was about 2700 s, and drift during the first eclipse was about 100 deg. This drift is larger than subsequent drift values, because the 250 N-m bias was not completely built up prior to the first eclipse. Drift during subsequent eclipses is seen to be less that 50 deg, with rapid recapture at entry to orbit day. Figure 6 shows the true body rates, which reveal a larger rate about *V*3 than around *V*1 and *V*2. This is mainly because Earth's magnetic field does not provide a true inertial reference, but rotates as HST moves through the field, as described above.

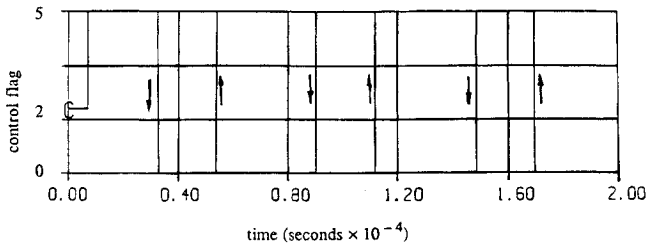

Fig. 4 Simulation results: control flag.

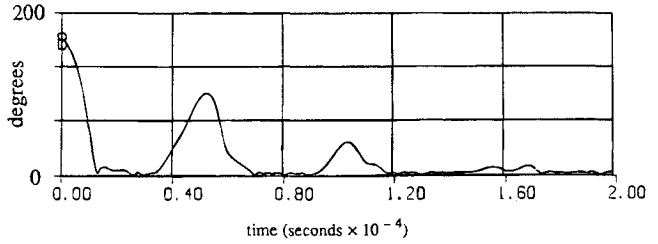

Fig. 5 Simulation results: angle between Sun and *V*3 axis.

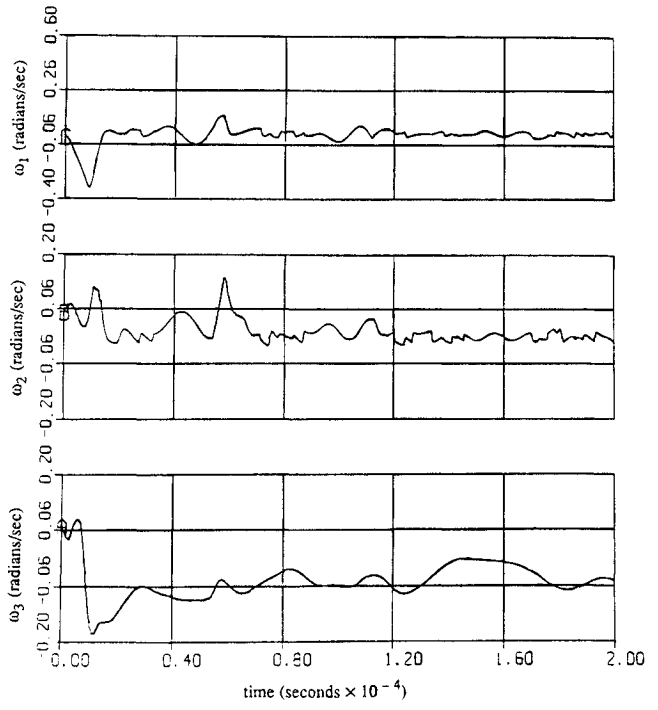

Fig. 6 Simulation results: true body rates.

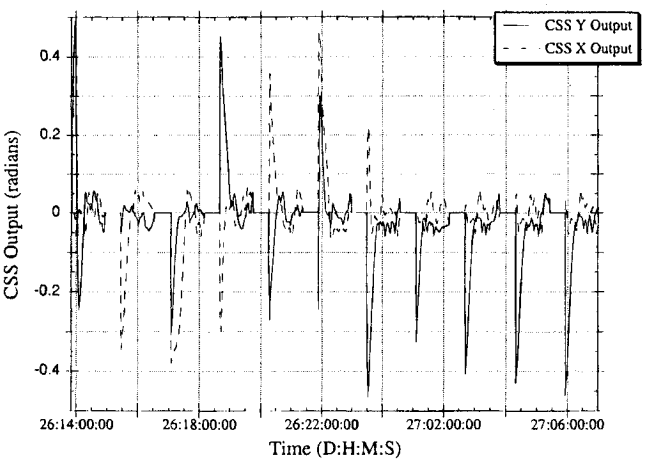

Fig. 7 On-orbit test: coarse Sun sensor outputs.

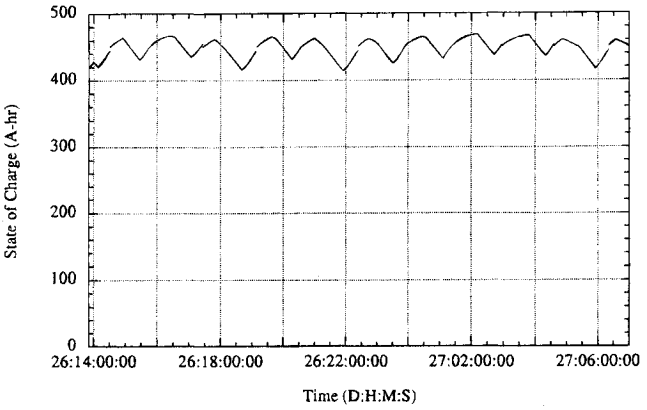

Fig. 8 On-orbit test: battery state of charge.

Table 1 On-orbit capture performance

Time, day/ h:min	Event	Initial *V*1 angle, deg	Initial *V*2 angle, deg	Capture time, min
26/13:50	Enter ZGSP	0.0	78.0	22
26/15:27	Enter Orbit Day	−19.8	−3.0	15
26/17:03	Enter Orbit Day	−21.7	−17.6	27
26/18:40	Enter Orbit Day	−16.4	23.4	20
26/20:16	Enter Orbit Day	20.5	−15.4	14
26/21:53	Enter Orbit Day	25.6	13.9	18
26/23:29	Enter Orbit Day	−0.4	−18.0	11
27/01:05	Enter Orbit Day	−0.4	−18.7	11
27/02:42	Enter Orbit Day	1.3	−23.4	13
27/04:19	Enter Orbit Day	2.8	−24.6	15
27/05:55	Enter Orbit Day	1.8	−27.0	17

Performance of −*V*1 ZGSP was also acceptable in all cases. The longest capture time was 5500 s. The second longest capture was 3000 s, and typical capture times were 1500–2000 s, even with large initial rates. Worst case drift during eclipse was largest during the first eclipse period, because reaction wheel momentum bias was not completely built up. Worst case drifts for the first, second, and third eclipses were 54, 43, and 40 deg, respectively. The largest wheel speed was 3000 rpm, with steady-state speeds around 2000 rpm.

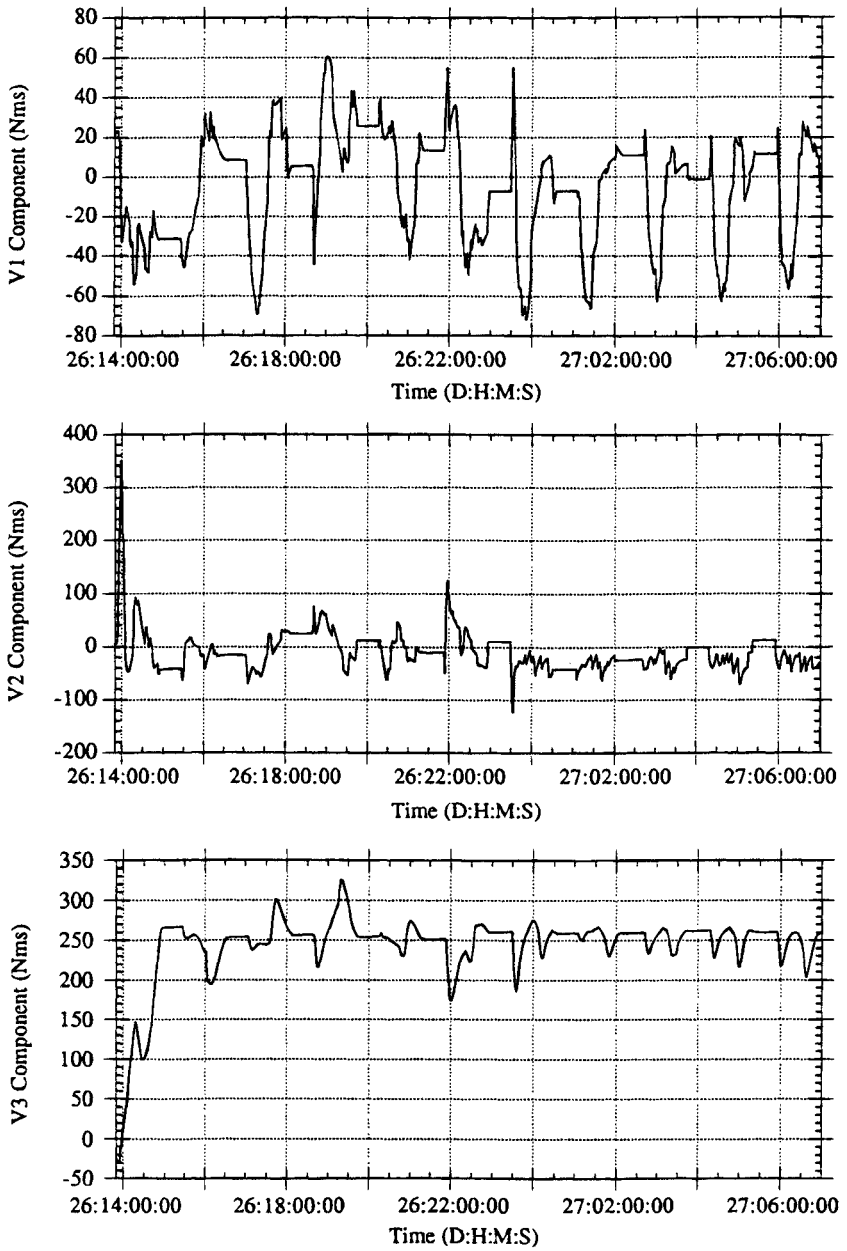

Fig. 9 On-orbit test: reaction wheel angular momentum.

Longer runs of 200,000 s (about 30 orbits or two days) were made to check the long-term stability of ZGSP; they showed good performance of both $V3$ and $-V1$ ZGSP.

On-Orbit Test Procedure

The $V3$ ZGSP safemode was successfully flight tested for 17 h on January 26–27, 1993. One purpose of the test was to verify the logic paths in the ZGSP code. A more critical purpose of the on-orbit test was to validate the models of spacecraft sensors, actuators, and hardware used in the ground simulations. Of particular concern were the aerodynamic torque, which is approximately modeled in the simulations and is one of the dominant contributors to attitude drift during eclipse, and the response of the CSS to glint and Earth albedo, which was not modeled in the simulations. The on-orbit procedures were carefully planned to minimize risk to the spacecraft while providing a meaningful test of the control mode. A combination of real-time commands and stored, time-tagged commands was employed to protect against the possible loss of communications with the ground (forward and/or return link) during the test.

The test began at 12:00 UTC (Universal Time Coordinated) on January 26 with HST in inertial hold mode at an initial attitude 78 deg from $V3$ sunpointing to give a realistic test of the acquisition performance. The aperture door was closed by independent ground command before entering the safemode to ensure proper door closure and to allow the test to be aborted in the unlikely event of aperture door failure. At 13:50 UTC, immediately after HST left the Earth's shadow (called Enter Orbit Day), a test macro (stored command sequence) was activated to force entry to ZGSP and set a stored time-tagged command to transition back to SWSP safemode after 150 min. This time was chosen to be long enough to allow evaluation of ZGSP performance, but short enough to avert damage to the spacecraft by any credible failure of the ZGSP safemode.

The performance of ZGSP for one orbit was evaluated from downlinked telemetry and was judged to be satisfactory, as

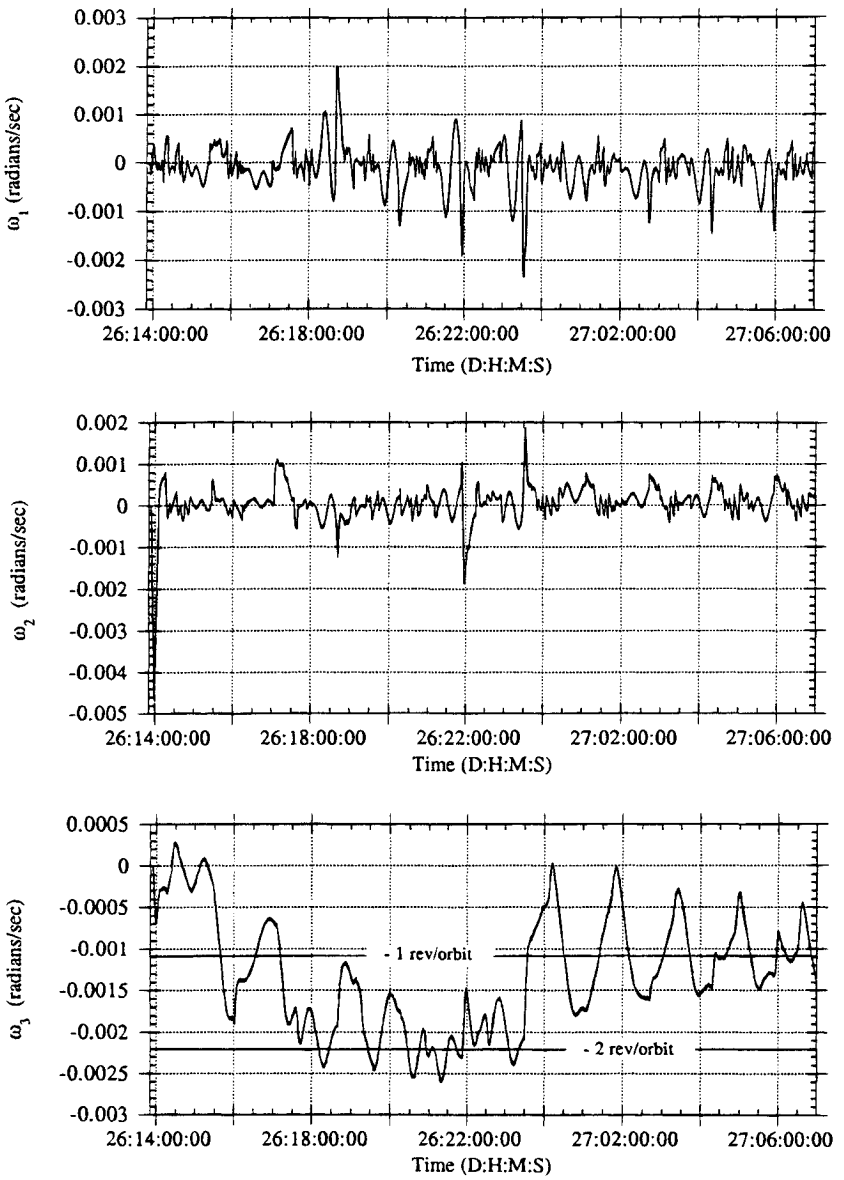

Fig. 10 On-orbit test: spacecraft angular velocity.

described below. If a problem had occurred during this period, the spacecraft could have been returned to SWSP safemode by real-time ground command. If sufficient evaluation data had not been available because of loss of return link, or if loss of forward link had precluded sending the real-time command, the stored command set by the test macro would have returned HST to SWSP safemode autonomously.

Because the first orbit of the ZGSP test was successfully completed, a second test macro was activated prior to the execution of the stored command set by the first test macro, resetting the timer in the special command processor to re-enter SWSP safemode after nine additional orbits. If a problem had occurred during these nine orbits, a real-time ground command would have been uplinked to return the spacecraft to SWSP control. The nine-orbit timer was chosen to provide a sufficient safety net after the successful completion of the first orbit in ZGSP safemode. In the event of an unanticipated failure endangering spacecraft health, existing autonomous safemode tests would have caused a transition to the hardware sunpoint capability using the Pointing and Safemode Electronics Assembly and recovery mode gyros.

Because the ZGSP safemode performed as expected, the test was allowed to continue for the full ten orbits, and recovery to SWSP control was begun at 7:00 UTC on January 27.

On-Orbit Test Performance

Figure 7 shows the outputs of CSS3, which is the coarse Sun sensor used for $V3$ sunpoint. This sensor is oriented so that the x output measures a spacecraft rotation about the $V1$ axis, while the y output measures the $V2$ excursion. Both outputs are zero during eclipse periods. Relatively large spikes in one or both CSS outputs are seen at each Enter Orbit Day, as well as at initial entry into ZGSP. The data on these entries and the subsequent captures are collected in Table 1. Except for the initial entry into ZGSP mode from a known attitude, the initial $V1$ and $V2$ angles are computed from the CSS outputs. The important column in the table is the last one, which contains

the capture times, defined as the times for both CSS signals to fall within 0.06 rads and remain there for the remainder of the sunlit portion of the orbit. The observed capture times are all well within the 30-min success criterion as well as in satisfactory agreement with the results of software simulations. They provide adequate solar array currents to keep the battery state-of-charge between 410 and 470 A-h, as shown in Fig. 8, providing a generous margin of safety.

Figure 9 shows the reaction wheel angular momentum during the ZGSP test. The $V1$ reaction wheel momentum is bounded by ± 75 N-m-s during the test. The $V2$ component of angular momentum shows a large initial peak caused by the initial 78 deg $V2$ maneuver, followed by a return to near zero values with deviations as required by the sunpointing control torques. The $V3$ component is commanded to a bias value of 250 N-m-s to maintain the sunpointing attitude during eclipse periods, as described above. The flight data in Figure 9 show how rapidly the magnetic torquing system establishes this desired bias angular momentum.

Figure 10 shows the spacecraft angular rates sensed by the gyros. These gyro-sensed rates are not used for ZGSP control, of course, but the telemetry was available for analysis of the on-orbit test. The $V1$ body rate shares with the $V1$ angular momentum the property of being the least interesting component. The $V2$ rate shows a large initial peak in the direction opposite to the peak in the corresponding component of the computed (reaction wheel) angular momentum. These oppositely directed peaks demonstrate the conservation of the true (reaction wheel plus body) system angular momentum, excepting the contributions of the relatively slowly acting environmental and magnetic control torques.

The most interesting component of the body rate is the $V3$ component, shown in Fig. 10. This has oscillatory behavior about -2 rev/orbit between 17:10 UTC and 23:30 UTC on January 26, in agreement with the rotation of the magnetic field vector described above. Before and after this time span, however, the motion shows larger and slower oscillations about a rate of -1 rev/orbit. This indicates that HST was exhibiting libration in a gravity-gradient null at these times, with the gravity-gradient torque overwhelming the low-gain magnetic rate damping.

The largest $V3$ rate during the test was -2.6×10^{-3} rad/s at 21:20 UTC on January 26. Because the spacecraft moment of inertia about the $V3$ axis is 7.8×10^4 kg-m^2, the peak $V3$ component of the body angular momentum is -203 N-m-s. This cancels most of the momentum bias in the reaction wheels, which is approximately 263 N-m-s at this time, resulting in an actual system momentum bias of only 60 N-m-s. The on-orbit test case was a worst case in terms of system momentum bias, because the body and reaction wheel momenta would have added rather than subtracted if the magnetic rate damping had resulted in oscillations about $+2$ rev/orbit. It is reassuring that this worst-case momentum bias provided adequate attitude stabilization during eclipse, in agreement with simulations.

Conclusions

A Zero-Gyro Sunpoint safemode, designed to ensure a power-positive state without the use of rate gyros, has been developed as a new layer of safemode for the Hubble Space Telescope. The new safemode uses coarse Sun sensors and magnetometers for attitude error and rate sensing, reaction wheels for attitude control, and magnetic torquers for momentum biasing and unloading. This new safemode was successfully tested on orbit on January 26–27, 1993. An initial sunpointing attitude error of 78 deg was reduced to 3 deg in less than 8 min following entry to the safemode. After some overshoot, the sunpointing error remained within 3 deg from 22 min after safemode entry until the spacecraft passed into Earth's shadow. The bias angular momentum along the Sun line, which is established to limit spacecraft attitude drift during eclipse, was attained during the first orbit. Reacquisition of sunpointing attitude to within 3 deg was attained in less than 30 min on all following re-entries of Hubble Space Telescope into sunlight, and the attitude remained within this limit during the remainder of the orbit day periods. The solar array currents were close to their maximum value for almost all of the daylight periods, and the state-of-charge of the batteries remained comfortably high. The on-orbit test results closely matched those of software simulations, validating the models of spacecraft sensors, actuators, and hardware used in the simulations.

The Zero-Gyro Sunpoint safemode was enabled by ground command on January 30, 1993, following evaluation of the test results. It can be entered by ground command or autonomously. Autonomous entry would result from a gyro failure evidenced by a rapid increase of computed system angular momentum, by a hardware failure indication, or by measured rates failing a disparity check or exceeding saturation limits. In the event of another gyro failure, the zero-gyro mode will allow Hubble Space Telescope to remain in a power- and thermal-safe condition until replacement of the failed rate gyro assemblies in the first servicing mission.

Acknowledgment

We acknowledge the invaluable contributions of Greg C. Andersen of Lockheed Technical Operations Co., Inc., in planning, performing, and evaluating the on-orbit test.

References

[1] Dougherty, H. J., Tompetrini, K., Levinthal, J., and Nurre, G., "Space Telescope Observatory in Space," *Journal of Guidance, Control, and Dynamics,* Vol. 5, No. 4, 1982, pp. 403–409.

[2] Dougherty, H. J., Rodoni, C., Rodden, J., and Tompetrini, K., "Space Telescope Pointing Control," *Astrodynamics 1983, Advances in the Astronautical Sciences, Vols. 54 I & II,* American Astronautical Society, 1983, pp. 619–630.

[3] Beals, G. A., Crum, R. C., Dougherty, H. J., Hegel, D. K., Kelley, J. L., and Rodden, J. J., "Hubble Space Telescope Precision Pointing Control System," *Journal of Guidance, Control, and Dynamics,* Vol. 11, No. 2, 1988, pp. 119–123.

[4] *HST Flight Software Detailed Design,* DM-04, Vol. III, Pt. 1, Lockheed Missiles and Space Company, Inc. Document LMSC/4173944Q, 25 Dec. 1991.

[5] *HST Flight Software Data Base,* DM-04, Vol. VI, Lockheed Missiles and Space Company, Inc. Document LMSC/4177611D, 2 Jan. 1992.

[6] Markley, F. L., and Nelson, J. D., "A Zero-Gyro Safemode Controller for HST," AIAA Paper 92-4613, Aug. 1992.

[7] *HST Pointing Control System Safing System Description Manual,* Lockheed Missiles and Space Company, Inc. Document LMSC/F256969, 12 Jan. 1990.

[8] Nelson, J. D., *Hubble Space Telescope Zero Gyro Sunpoint Analysis,* Lockheed Missiles and Space Company, Inc. Document LMSC/P015661, 26 Feb. 1992.